Available online at www.sciencedirect.com

ScienceDirect

Developmental Biology 303 (2007) 281–294

DEVELOPMENTAL BIOLOGY

www.elsevier.com/locate/ydbio

The left–right axis is regulated by the interplay of Coco, Xnr1 and derrière in *Xenopus* embryos

Alin Vonica, Ali H. Brivanlou *

The Laboratory of Vertebrate Embryology, The Rockefeller University, New York, NY 10021, USA

Received for publication 9 June 2006; revised 15 September 2006; accepted 20 September 2006
Available online 28 September 2006

Abstract

Formation of the left–right axis involves a symmetry-breaking signal originating in the node or its equivalents, which increases TGF-β signaling on the left side of the embryo and ultimately leads to asymmetric patterning of the viscera. DAN domain proteins are extracellular inhibitors of TGF-β ligands, and are involved in regulating the left–right axis in chick, mouse and zebrafish. We find that Coco, a *Xenopus* DAN family member, and two TGF-β ligands, Xnr1 and derrière, are coexpressed in the posterior paraxial mesoderm at neurula stage. Side-specific protein depletion demonstrated that left–right patterning requires Coco exclusively on the right side, and Xnr1 and derrière exclusively on the left, despite their bilateral expression pattern. In the absence of Coco, the TGF-β signal is bilateral. Interactions among the three proteins show that derrière is required for normal levels of *Xnr1* expression, while Coco directly inhibits both ligands. We conclude that derrière, Xnr1, and Coco define a posttranscriptionally regulated signaling center, which is a necessary link in the signaling chain leading to an increased TGF-β signal on the left side of the embryo.

Keywords: Coco; Xnr1; Derrière; Left–right; Asymmetry; *Xenopus*; Paraxial

Introduction

The role of the TGF-β pathway in establishing the left–right axis has long been established in *Xenopus*. In normal left–right patterning, TGF-β ligands in the left lateral plate mesoderm (LPM) activate secondary signaling events that determine the asymmetric development of mesodermal and endodermal organs such as the heart and gut. Ectopic right side activation of TGF-β signaling by overexpression of *Xnr1* (Sampath et al., 1997), *activin* and *Vg1* (Hyatt and Yost, 1998; Hyatt et al., 1996), *derrière* (Hanafusa et al., 2000), and TGF-β5 (Mogi et al., 2003) randomizes, or in some cases switches, the left–right axis. Conversely, inhibition of TGF-β signaling on the left side through use of dominant negative constructs of TGF-β receptors type II ActRIIb (Hemmati-Brivanlou and Melton, 1992) and type I Alk4 (Chang et al., 1997), and of the ligand derrière (Hanafusa et al., 2000) produces the same effect of left–right randomization. Nevertheless, the in vivo role of individual ligands is difficult to determine because overexpression produces overlapping effects. For instance, wild-type derrière can heterodimerize with other TGF-β ligands, and the dominant negative mutant interferes with all nodal-like signals in the early *Xenopus* embryo (Eimon and Harland, 2002).

The only *Xenopus* nodal gene asymmetrically expressed is *Xnr1* in the left LPM (Lohr et al., 1997; Lustig et al., 1996; Sampath et al., 1997), which induces other asymmetric genes, like the nodal antagonists *Xlefty-a* (Branford et al., 2000) and *Xatv* (Cheng et al., 2000), and the transcription factor *Pitx2c* (Schweickert et al., 2000). These genes constitute a conserved signaling network that patterns the left–right axis in vertebrates (reviewed in Bisgrove and Yost, 2001; Brand, 2003; Levin, 2005; Wright, 2001).

Members of the DAN family of secreted proteins (Avsian-Kretchmer and Hsueh, 2004; Hsu et al., 1998; Pearce et al., 1999), defined structurally by the presence of a specific cysteine knot domain, have also been implicated in left–right axis determination. Biochemically, all DAN domain proteins inhibit BMP-type TGF-β ligands, and two factors, originally found in *Xenopus*, can also inhibit nodal signaling, Cerberus (Hsu et

* Corresponding author. Fax: +1 212 327 8685.
E-mail address: brvnlou@rockefeller.edu (A.H. Brivanlou).

0012-1606/$ - see front matter © 2006 Elsevier Inc. All rights reserved.
doi:10.1016/j.ydbio.2006.09.039

al., 1998; Piccolo et al., 1999), the orthologue of mouse Cer1/Cerberus-like/Cerr1/cer-1, human CER1/DAND4 and chick CER1/Caronte, and Coco (Bell et al., 2003), the orthologue of mouse Dand5/coco/Dte/Cerl-2 and human DAND5/DANTE/GREM3/CER2/DTE/CKTSF1B3. The first indications of a role in left–right axis came from chick, *CER1*/*Caronte*, expressed in the paraxial mesoderm and the left LPM, was hypothesized to antagonize BMP and thus permit *nodal* expression (Rodriguez Esteban et al., 1999; Yokouchi et al., 1999; Zhu et al., 1999). Recent reports, however, assign a positive function for BMPs in the left LPM in chick (Piedra and Ros, 2002; Schlange et al., 2002), thus questioning the previously assigned targets of CER1/Caronte. Work in mouse and zebrafish (Hashimoto et al., 2004; Marques et al., 2004; Pearce et al., 1999) has now shown that DAN family genes, expressed in the posterior mesoderm around the node in mouse (*Dand5/Cerl-2/Dte*) or Kupffer's vesicle in fish (*Charon*), are necessary for normal left–right asymmetry. The mouse knock-out and the fish protein depletion randomize the left–right axis as a consequence of bilateral expression of laterality genes like *nodal* (*southpaw* in fish), *lefty*, and *Pitx2* in the LPM. In zebrafish, the gene encoding a nodal ligand (*southpaw*) is epistatic to *Charon*, suggesting that Nodal inhibition in the posterior paraxial mesoderm is the mechanism for the Charon effect. In mice, the importance of early *nodal* expression around the node was demonstrated by conditional knock-out and a hypomorphic mutation (Brennan et al., 2002; Saijoh et al., 2003).

We report here that the DAN domain protein Coco (Bell et al., 2003) has an essential role in regulating the left–right axis in *Xenopus laevis*. A detailed in situ analysis showed that *Coco* is expressed bilaterally in the posterior paraxial mesoderm, where it overlaps with the TGF-β ligands *Xnr1* and *derrière*. Knock-down of Coco protein randomizes visceral asymmetry as a result of bilateral LPM expression of laterality genes. The Coco protein is required exclusively on the right side of the embryo, while Xnr1 and derrière are exclusively required on the left. Both TGF-β ligands are epistatic to Coco, and we also show that derrière, like Xnr1, is an in vitro target of Coco inhibition. We conclude that Coco regulates the left–right axis by blocking a TGF-β cascade in the right posterior paraxial mesoderm.

Materials and methods

Design of antisense morpholino oligonucleotides and plasmid construction

For Coco antisense morpholino oligonucleotide (MO) design, we checked the *Xenopus* EST databases for presence of a Coco-related sequence. We found a *Coco* allele that we name *Coco2* (CA981167), which has 63% identity over the whole cDNA sequence, and 91% identity to Coco in the amino acid sequence. The antisense MOs Coco1 MO 5′ CTG GTG GCC TGG AAC AAC AGC ATG T 3′, and Coco2 MO 5′ TGG TGG CCT GGA ACA GCA GCA TGT C 3′, were complementary to *Coco* and *Coco2*, respectively, and covered sequences that differed by a single nucleotide. The two MOs were functionally equivalent, and were used together as Coco MO. The Coco Mut MO, used as specificity control, had 5 point mutations (small case): 5′ CTG Ctg GCg TCC AtC AAg AGC TtG T 3′. For *Xnr1*, we designed the antisense Xnr1 MO 5′ GCT GTC AGA AAT GCC ATG CTT GCA C 3′ and Xnr1 Mut MO with 5 point mutations (in small case) 5′ GCT cTC AcA AAT cCC ATc CTT cCA C 3′. For *derrière*, we found the allelic sequence BC073508, which diverged in the 5′ UTR from the original sequence (AF065135) but was conserved around the start ATG. We designed the antisense Der MO, 5′ CAC AAC TCT GCC ATG TTG ACT TCT C 3′, and Der Mut MO with 5 point mutations (small case), 5′ CAg AAC TgT GCg ATG TTc ACT TgT C 3′.

To construct a *Coco* expression vector resistant to MO inhibition, pCS2+ *Mut Coco*, we amplified *Coco* by PCR, and introduced a 3′ end FLAG tag and the following mutations (mutated nucleotides in small case: 5′ CAT GtT acT cTT tCA aGC 3′). To construct pCS2+ *GRVP16hSmad2Δ3*, we first amplified *hSmad2Δexon3* as 5′ HA-tagged fragment from pc def3 FLAG-*Smad2 Δexon3* (Yagi et al., 1999) by PCR, then cloned it as *Xho*I/*Xba*I fragment into pCS2+. The *Xho*I/*Not*I fragment, containing *hSmad2Δ3*, was then moved to ΔβTG (Darken and Wilson, 2001), which contains the glucocorticoid binding domain of the glucocorticoid receptor, amino acids 512–777. The VP16 activation domain (amino acids 411–490) was amplified by PCR from pCS2-VP16ΔβXtcf-3 (Vonica et al., 2000) and inserted as *Eco*RI/*Xho*I fragment in the above vector.

RNA preparation

RNA for injections was prepared using the mMessage mMachine in vitro SP6 transcription kit (Ambion). In addition to the vectors described above, we used pCS2 ++FLAG*Coco* (Bell et al., 2003), pCS2 proAct-HA-*Xnr1* (from E. De Robertis), pCS2 proAct-HA-*derrière* (from R. Harland), and SP6 *nucβGal* (from R. Harland). Antisense probes for in situ hybridization were synthesized with digoxigenin (Dig) or with fluorescein (FITC) labeling mix (Roche) for the *LacZ* probe.

Embryo culture and injections, immunohistochemistry, immunofluorescence, and in situ hybridization

In vitro fertilized embryos were cultured in 0.1xMMR and injected as indicated. Embryos were staged according to Nieuwkoop and Faber (1967). Heart and gut inversions were scored at stage 46 like in Branford et al. (2000), but the different abnormal gut patterns were scored together. Immunohistochemistry and immunofluorescence for heart muscle were performed with mouse monoclonal antibodies to bovine cardiac troponin T (from the Developmental Studies Hybridoma Bank at the University of Iowa), as described (Kolker et al., 2000). Confocal immunofluoresce was performed with a Zeiss confocal microscope and Pascal software. The Z-stack obtained from confocal microscopy was compressed to a single layer along the *X* axis before transferring to Adobe Photoshop. Whole-mount in situ hybridization was as described (Harland, 1991), with full-length probes transcribed from the following vectors: pCS2++*Coco* (Bell et al., 2003), pBS *Xnr1* and pBS *Xlefty-a* (Branford et al., 2000), pBS *Xnr2* (BG023015, from ATCC), pBS *Xnr5* and pBS *Xnr6* (Takahashi et al., 2000), pCMV-SPORT6 *derrière* (CA789921, from ATCC), Topo *Pitx2c* (Schweickert et al., 2000), pBS *Zic3* (Kitaguchi et al., 2000), pBS *XShh* (Ruiz i Altaba et al., 1995), and pSP6 *nucβGal* for *LacZ* in situ. To reduce background stain, for *Xnr1* probes stringency was increased by raising temperature to 65°C for 2× SSC washes, and by adding 0.3% CHAPS. For double in situ hybridization, we used a Dig-labeled probe for the marker genes, and a FITC-labeled *LacZ* probe for the tracer. The Dig probe was stained with BM Purple, and the FITC probe with FAST Red (Roche). Embryos were cleared in benzyl benzoate-benzyl alcohol mix (Sive et al., 1997). Sections of whole mounts were performed on agarose-embedded embryos with a vibratome. For in situ hybridization of paraffin sections, fixed embryos were embedded in paraffin, sectioned at 15-μm thickness, deparaffinized, and consecutive slides were subjected to in situ hybridization with digoxigenin-labeled *Coco* or *Xnr1* probes and stained with BM Purple (Neubuser et al., 1995). Digital pictures were minimally enhanced in Adobe Photoshop 7.0 imaging program. To obtain an overlap of two pictures, stained areas were selected and their color changed, and the overlaying picture was rendered partially transparent.

RT-PCR and transcription assays

For RT-PCR, animal caps from embryos injected in the animal pole with the indicated RNAs were dissected at stage 9 and cultured in 0.5× MMR. For the

posterior paraxial expression assay, MOs were injected in each dorsal blastomere of four-cell stage embryos, and a dorsal posterior fragment, containing axial and paraxial mesoderm and the adjacent neuroectoderm, was dissected at stage 18. For dorsal expression of *Xnr1* in Der MO-injected embryos, the dorsal marginal zone was recovered at stage 10+. Each batch, containing 5 caps or 10 posterior/dorsal fragments, was processed as described (Wilson and Melton, 1994). One of three experiments is shown in each case. *ODC* was used as loading control. The primers used were: *Xnr1* sense 5′ TAA AAG CAA AGG AAA GGG CAG AG 3′, antisense 5′ GAT GCT TCC TAT TGA TAA GTG ATG 3′; *Xnr2* sense 5′ TTG TTC TTC GTC ATT GCT TCC CT 3′, antisense 5′ CCT TGA TGG AGA TAA TAC TGG AG 3′; *Xnr5* sense 5′ CAC ACA GAC TGG AAC CTT CAC C 3′ antisense 5′ GTG TCA CAT TCT GGA ACC TCT G 3′; *Xnr6* 5′ GTG GCA CTG AGA CCA TCT ACT AG 3′, antisense 5′ CAG GAA GAA GTT CTC GTG ACG G 3′; *derrière* sense 5′ TGG CAG AGT TGT GGC TAT CA 3′, antisense 5′ CTA TGG CTG CTA TGG TTC CTT 3′; *Coco2* sense 5′ GCA CTT CCT GCG CTC CTA GCC 3′, antisense 5′ CTT TGG AGG CCC GCC GGG TCC 3′; *XBra* sense 5′ GGA TCG TTA TCA CCT CTG 3′, antisense 5′ GTG TAG TCT GTA GCA GCA 3′; *ODC* sense 5′ CGA AGG CTA AAG TTG CAG 3′, antisense 5′ AAT GGA TTT CAG AGA CCA 3′. For transcription assays, the nodal/activin-specific reporter gene A3Luc (Liu et al., 1997) was coinjected with the inducible Smad2 construct *GRVP16hSmad2Δ3* RNA in the animal pole at four-cell stage. Embryos were cultured in the presence or absence of 1 μM dexamethasone until stage 11, when they were processed for luciferase assays (Promega) as described (Vonica and Gumbiner, 2002). All assays were done in triplicate.

In vitro translation

RNAs for full-length, wild-type *Coco*, *Xnr1* and *derrière* were transcribed from pCS2++*Coco*, pBS *Xnr1* and pCMV-SPORT *derrière*, and the mutated *Coco* was transcribed from pCS2+*Mut Coco*. The RNAs (1 μg) were translated in the presence of [S^{35}]Met with the Rabbit Reticulocyte Lysate System (Promega), with or without addition of MOs (Taylor Kobzik JBC 96).

Western blots and immunoprecipitation

For Coco Western, embryos injected in animal poles at the four-cell stage with full-length wild-type *Coco* or *Mut Coco* RNA, alone or together with MOs, were collected at stage 11 and lysed in 1% NP-40 buffer. PAGE-SDS gels were run on Invitrogen 4–12% precast gels. Western blots were incubated with an antibody raised in rabbits against the C-terminal Coco peptide TRYDRNTVEPAGSGEDYLPVS at a concentration of 1:500 for endogenous and 1:10,000 for overexpressed Coco, or with N-terminal anti-β-catenin antibody (from B. Gumbiner) at 1:10,000. The antibody specifically recognized a band of the correct size only in embryos injected with *Coco* RNA. For endogenous Coco expression in control embryos injected with 3 ng Control MO and in embryos injected dorsally bilaterally with 3 ng Coco MO, posterior dorsal fragments containing axial and paraxial mesoderm were dissected at stage 18 (100 for each lane), and samples were run on a large BioRad gel. For immunoprecipitation, *HA-Xnr1*, *HA-derrière* and *FLAG-Coco* RNAs were injected in the animal poles of four-cell stage embryos. At stage 9, caps were collected by manual dissection in calcium-free medium (CMFM), and placed in 96-well plates in the same buffer overnight at 13°C (100 μl medium/10 caps). Medium was collected, diluted in immunoprecipitation buffer (Piccolo et al., 1999) to a volume of 500 μl, and subjected to immunoprecipitation with anti-FLAG M2 beads (Sigma). Western blots of bead-bound proteins were performed with rabbit polyclonal antibodies against the HA (Upstate Cell Signaling Solutions) and FLAG tags (Sigma), 1:1000 dilution.

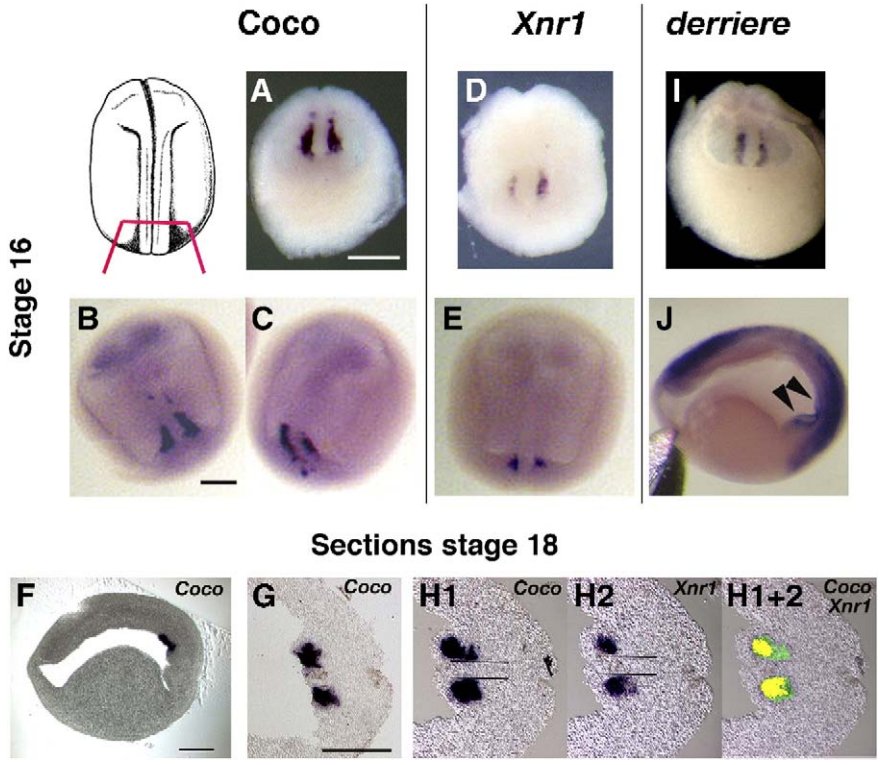

Fig. 1. *Coco*, *Xnr1* and *derrière* are coexpressed in *Xenopus* neurula. In situ hybridization for *Coco* (A–C, F, G, H1), *Xnr1* (D, E, H2), and *derrière* (I, J). Panels A, D, I are inner views of posterior fragments, dorsal side up, dissected as shown in the drawing on upper left (dorsal view, anterior is up); B, C, E are cleared whole embryos, dorsal views, posterior side down; J is a cleared embryo, lateral view, anterior to the left; F is a paraxial longitudinal section of a whole-mount in situ stained embryo, G–H2 are in situ hybridizations of horizontal paraffin sections. Panels H1 and H2 are consecutive sections (15 μm thick), and H3 is an overlap of H1 and 2, with false color for *Coco* (green) and *Xnr1* (red), and the overlap (yellow). Horizontal lines in H1 and H2 indicate the lateral borders of the notochord. The lower arrowhead in panel J shows the most posterior segment of *derrière* expression. Scale bars panels in A and B represent 0.2 mm.

Results

Coco, Xnr1 and derrière are coexpressed in the posterior paraxial mesoderm of Xenopus neurula

Our previous work described the maternal and early zygotic pattern of *Coco* expression. After gastrulation (stage 11, Nieuwkoop and Faber, 1967), *Coco* RNA decreases abruptly to a low level, which is maintained into tadpole stages (Bell et al., 2003). We investigated the localization of this late *Coco* expression from stage 12 by in situ hybridization (end of gastrulation). *Coco* became detectable on the inner side of the dorsal lip of the blastopore from stage 13, in discrete bilateral streaks (not shown). Expression increased in intensity (Figs.

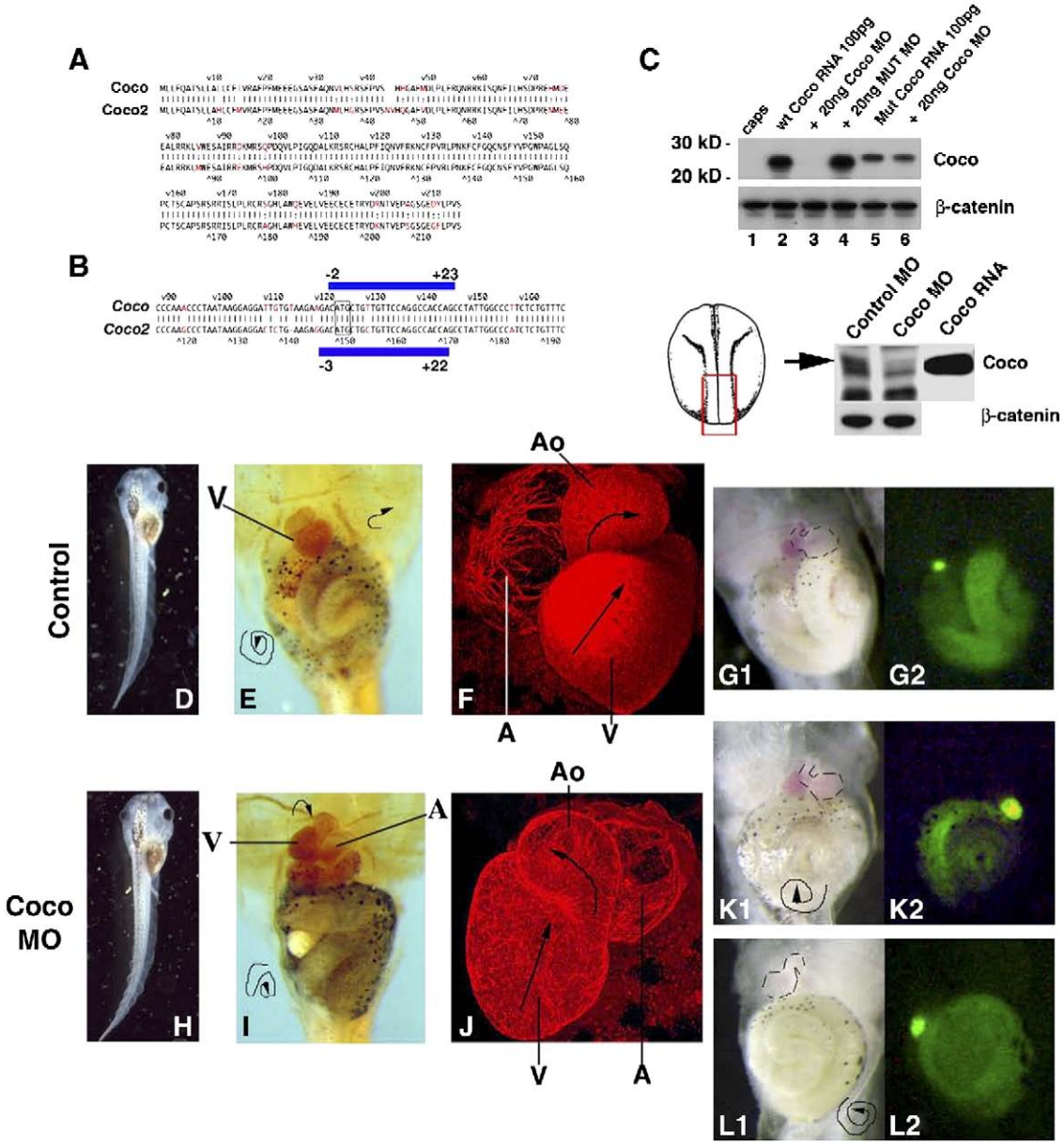

Fig. 2. Depletion of Coco protein randomizes the left–right axis. (A) Alignment of the Coco and Coco2 sequences. (B) Design of Coco MO1 and 2. A mix of both was used. (C) Coco MO specifically inhibits translation of injected and endogenous wild-type *Coco* RNA but not of a 5′ mutated RNA (*Mut Coco*). Western blots. Upper panel. 100 pg *Coco* or *Mut Coco* RNA were injected in the animal pole of each blastomere at the two-cell stage, alone (lanes 2, 5) or with 20 ng of either Coco MO (lanes 3, 6) or Coco Mut MO (lane 4). Animal caps were collected at stage 10. Coco protein was detected with anti-Coco antibody (1:10,000). Lower panel. Expression of endogenous Coco protein is inhibited by Coco MOs. The diagram represents a neurula-stage embryos, dorsal view, with the dissected dorsal posterior fragment boxed. Each lane contains 100 dissected dorsal posterior fragments (stage 18) from embryos injected dorsally with 3 ng control MO or 3 ng Coco MO. Positive control was overexpressed Coco FLAG RNA. Polyclonal antibodies for Coco (1:500) and β-catenin (1:10,000) were used. (D–L) Stage 46 embryos, dorsal (whole, D, H) and ventral (details) views. (D–G) Control embryos. (H–L) Embryos injected at four-cell stage in the dorsal right blastomere with 3 ng Coco MO. (E, I) Immunohistochemistry (peroxidase), (F, J) immunofluorescence for cardiac troponin. V: ventricle; A: atrium; Ao: aorta. Curved arrows indicate the direction of the outflow tract and of the gut looping, straight arrows in panels F and J indicate the antero-posterior axis. Panel I is a complete inversion (Situs inversus), panel K is an isolated gut inversion and panel L is an isolated heart inversion (Situs ambiguus). Hearts are contoured in panels G1, K1 and L1, and G2, K2, and L2 show the position of the gall bladder by UV autofluorescence in the same embryos.

Table 1
Phenotypes of Coco MO-injected embryos

Injection	Amount MO (ng MO)	Injection site	Situs solitus (%)	Situs ambiguus (%)	Situs inversus (%)	Total injected
Control	0		96	4	0	146
Coco MO	3	Right dorsal	36	37	27	151
CocoMO+CocoRNA	3	Right dorsal	68	23	9	62
Coco Mut MO	3	Right dorsal	92	8	0	53

Coco RNA (10 pg injected) was a 5′ mutated *Coco* variant. Injections were done at four-cell stage.

1A–C) until stage 20, then decreased until disappearing at stage 24 (not shown). Both symmetric and asymmetric patterns were noticed (stronger on the left in Fig. 1C, symmetric in panel A, stronger on the right in panel B), suggesting a dynamic expression pattern. Histological sections of stage 18 embryos stained by whole-mount in situ hybridization (Figs. 1F, G) showed that *Coco* expressing cells are on the ventral side of the paraxial mesoderm, in contact with the archenteron. In sections capturing more anterior territory, *Coco* was separated from the archenteron by a layer of endoderm (Fig. 1H1). The difference between the anterior (G) and posterior (H) sections is explained by the zipper-like closure of the endoderm over the mesoderm of the archenteron roof in an anterior-to-posterior direction (Shook et al., 2004). In conclusion, *Coco* is expressed in the posterior paraxial mesoderm, adjacent to the notochord, from stages 13 to 24.

The posterior paraxial mesoderm was reported to express *Xnr1* (Lohr et al., 1998; Lustig et al., 1996), the *Xenopus* homologue of mouse *nodal* (Collignon et al., 1996; Conlon et al., 1994; Zhou et al., 1993) and zebrafish *southpaw* (Long et al., 2003), at tadpole stage. We detected *Xnr1* expression in the posterior paraxial mesoderm as early as stage 16 (Figs. 1D, E), and, similar to *Coco*, it was either asymmetric without a systematic bias for the left or the right side, or bilaterally symmetric. Our early timing for *Xnr1* expression confirmed a recent report (Onuma et al., 2005).

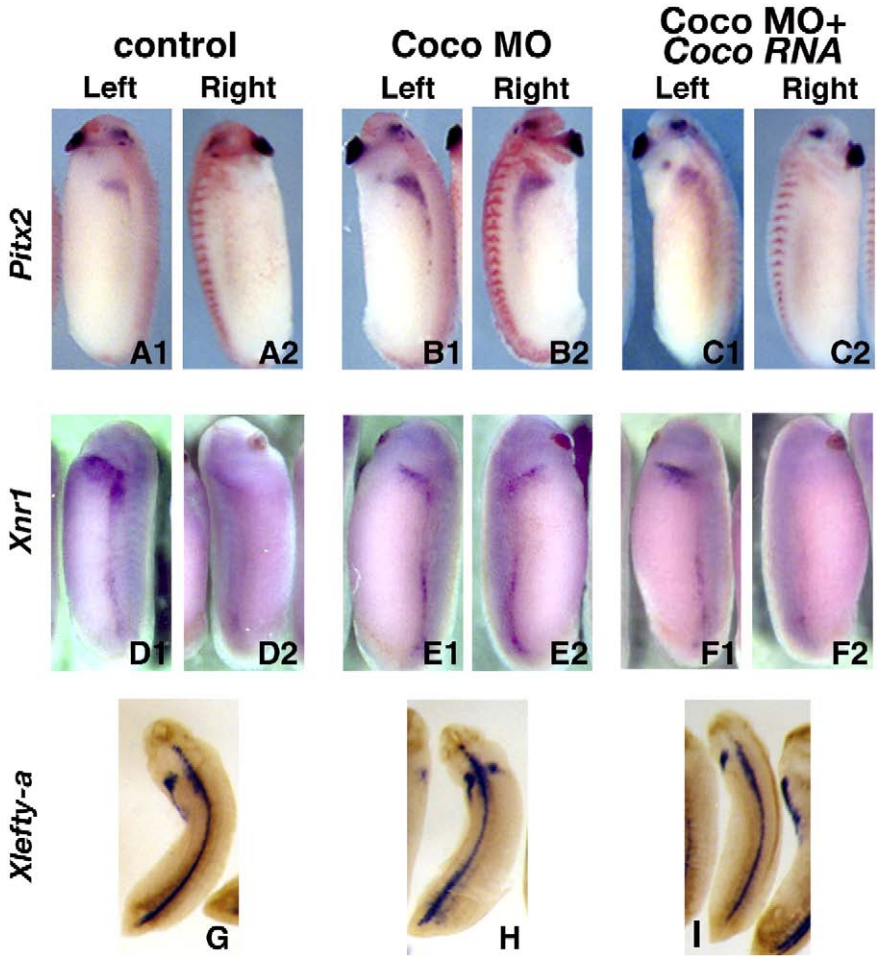

Fig. 3. The effect of Coco MO on asymmetrically expressed genes. Stage 25–26 embryos were stained by in situ hybridization for *Pitx2c* (A–C), *Xnr1* (D–F), and *Xlefty-a* (G–I). Left and right sides of the same embryos are shown. Panels G–I are dorsal views of cleared embryos, showing midline expression of *Xlefty-a*. Embryos injected in the right dorsal blastomere with 3 ng Coco MO have mostly bilateral expression of *Pitx2c* (B), *Xnr1* (E), and *Xlefty-a* (H). Coinjection of *Mut Coco* RNA (10 pg) restores left-side expression in Coco MO-injected embryos (*Pitx2c* C, *Xnr1* F, *Xlefty-a* I). Panels A, D, G are controls. Embryos in panels A–C were coinjected with 1 ng *LacZ* RNA and stained with Red Gal, to show that the right side was correctly targeted.

Table 2
Expression of laterality markers *Pitx2c*, *Xnr1* and *Xlefty-a* in Coco MO-injected embryos

Injection	Amount MO (ng MO)	Injection site	Normal (%)	Bilateral (%)	Inverted (%)	Total injected
Pitx2c						
Controls	0		100	0	0	23
Coco MO	3	Right dorsal	2	87	11	46
CocoMO+CocoRNA	3	Right dorsal	85	15	0	20
Coco Mut MO	3	Right dorsal	96	0	4	26
Xnr1						
Controls	0		100	0	0	46
Coco MO	3		24	68	8	51
CocoMO+CocoRNA	3		73	20	7	40
Xlefty-a						
Controls	0		100	0	0	18
Coco MO	3		30	30	40	20
CocoMO+CocoRNA	3		70	30	0	20

Coco RNA (10 pg injected) was a 5′ mutated *Coco* variant. Injections were done at four-cell stage. Normal expression for all markers (indicated in bold first column) is in the left lateral plate mesoderm.

Paraxial expression was maintained after stage 24, when *Coco* expression was turned off, and expression in the left LPM was detected from stage 20 (not shown). In situ hybridization with probes for *Coco* and *Xnr1* on consecutive horizontal sections (Figs. 1H1, H2, overlapped in H3: green for *Coco*, red for *Xnr1*, yellow for overlap) showed that the two genes are coexpressed.

Interestingly, we tested multiple TGF-β ligands by in situ hybridization and found that *derrière* is also expressed in the posterior paraxial mesoderm (Figs. 1I, J) from stage 12 to stage 20 (not shown), in addition to its ectodermal expression around the blastopore and the lateral edges of the neural plate (Hanafusa et al., 2000; Sun et al., 1999). *derrière* extended to a more posterior location than either *Coco* or *Xnr1* (Fig. 1J, lower arrowhead), but displayed similar lack of bias between the left and right side (not shown).

Our in situ analysis indicates that *Coco*, *Xnr1* and *derrière* are coexpressed bilaterally in the posterior paraxial mesoderm. Expression of *Coco* and *Xnr1* is comparable to expression of their homologues around the node in the mouse and the Kupffer vesicle in zebrafish. *derrière* is expressed first from stage 12, followed by *Coco* from stage 13 and *Xnr1* from stage 16. The order of appearance of the genes is maintained in the order of their disappearance.

Depletion of the zygotic Coco protein randomizes the left–right axis

To uncover the zygotic function of Coco in vivo, we designed morpholino oligonucleotides (MO) to interfere with the translation of endogenous Coco RNA (Fig. 2). Using the BLAST algorithm (Altschul et al., 1990) to search for sequences similar to Coco, we found a *Coco* allele (accession number CA981167), which we named *Coco2*, encoding a protein 91% identical to the original Coco protein (Fig. 2A). This gene shares the same expression pattern with *Coco* by RT-PCR (data not shown). The two MO designed (Fig. 2B) differed by only one nucleotide and were equally effective in vivo. When injected in the animal pole of *Xenopus* embryos, Coco MO inhibited translation from coinjected wild-type *Coco* RNA (Fig. 2C, upper panel, lanes 2, 3), but not from an RNA with mutations in the 5′ region of the open reading frame (*Mut Coco*, Fig. 2C lanes 5, 6). Both the wild-type and mutant Coco proteins were detected with a polyclonal antibody raised against a C-terminal peptide. The specificity of the Coco MO was further demonstrated by a MO containing 5 point mutations (Coco Mut MO), which had no effect on the translation of wild-type *Coco* RNA (Fig. 2C lane 4). Endogenous Coco protein was detected in posterior dorsal fragments of stage 18 embryos as a band migrating at the same level with overexpressed wild-type Coco protein (Fig. 2C, lower panel), and was equally expressed on the right and left side (data not shown). Bilateral injections of Coco MOs produced a marked decrease in Coco protein levels (Fig. 2C, lower panel).

Depletion of Coco protein with Coco MO resulted in randomized left–right axis (Figs. 2H–L, Table 1), in the absence of other changes in head and body patterning (Fig. 2, D wild-type, H complete inversion), or of effects on posterior paraxial expression of *Xnr1*, *derrière* (Figs. S4 B, E), and

Table 3
Comparison of the left and right side effects of Coco MO and Coco RNA

Injection	Amount MO (ng MO pg RNA)	Injection site	Situs solitus (%)	Situs ambiguus (%)	Situs inversus (%)	Total injected
Controls	0		100	0	0	51
Coco MO	3	Right dorsal	28	38	34	39
Coco MO	3	Left dorsal	88	12	0	34
Coco RNA	10	Right dorsal	81	13	6	31
Coco RNA	10	Left dorsal	17	48	35	69

Injections were done at four-cell stage in the indicated blastomere.

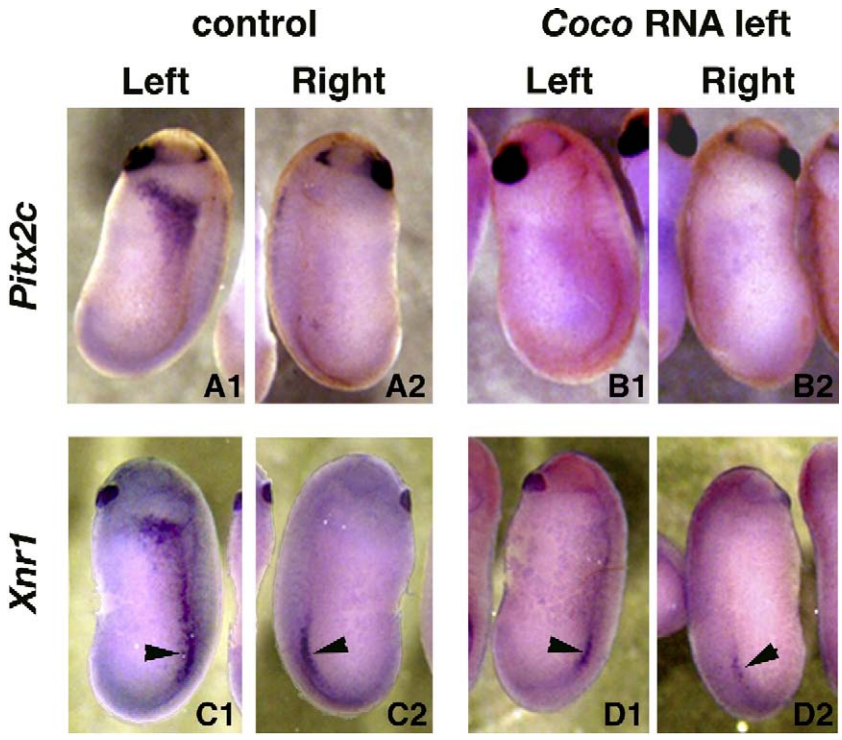

Fig. 4. *Coco* RNA prevents expression of left side markers. Embryos were injected on the left dorsal side of four-cell stage embryos with *Coco* RNA (10 pg) and collected at stage 24. In situ hybridization for *Pitx2c* (A, B) and *Xnr1* (C, D). Left and right sides of the same embryos are shown. Arrowheads in panels C and D indicate the posterior, bilateral expression domain of *Xnr1*, not affected by *Coco* RNA.

Coco itself (not shown). The asynchronous looping of the heart and gut produced embryos with normal (Situs solitus), mixed (isolated heart or gut inversion, Situs ambiguus, Figs. 2K1, L1), or inverted (heart and gut inverted, Situs inversus, Fig. 2I) position of the viscera. This phenotype was observed with high penetrance in both bilateral dorsal and right dorsal injections of four-cell stage embryos. Visualization of the heart with cardiac muscle antibody (Figs. 2E, I, immunoperoxidase, F, J confocal immunofluorescence), as well as UV detection of the gall bladder (Figs. 2G2, K2, L2) confirmed the phenotype. This effect was specific, as it could be rescued by coinjection of a mutated *Mut Coco* RNA (68% normal embryos, compared to 36% for embryos injected with Coco MO, Table 1), and the fact that a mutant MO (Coco Mut MO) did not elicit the phenotype (96% normal embryos).

To address the molecular basis for the phenotype of Coco depleted embryos, we stained laterally expressed genes by in situ hybridization (Fig. 3, Table 2). *Xnr1* (Lohr et al., 1997; Lustig et al., 1996; Sampath et al., 1997), *Xlefty-a* (Branford et al., 2000), and *Pitx2c* (Schweickert et al., 2000) are all expressed in the left LPM at tadpole stage. Embryos injected with Coco MO in the right dorsal blastomere at the four-cell stage had mostly bilateral, sometime inverted expression of *Pitx2c* (Fig. 3B, Table 2), *Xnr1* (Fig. 3E), and *Xlefty-a* (Fig. 3H). Coinjection of *Mut Coco* RNA partially restored the normal expression pattern (*Pitx2c* normal pattern increased from 2% with Coco MO alone to 85%, Fig. 3C and Table 2, *Xnr1* from 24% to 73%, Fig. 3F, and *Xlefty-a* from 30% to 70%, Fig. 3I). Coco Mut MO had little effect on *Pitx2c* expression (Table 2). To exclude the possibility of left–right axis defects as a result of midline anomalies (Kitaguchi et al., 2000; Lohr et al., 1997), we verified the midline expression of *Xlefty-a* (Fig. 3I), *Xshh* (Ekker et al., 1995) and *Zic3* (Kitaguchi et al., 2000) (results not shown), all of which were normal. The predominantly bilateral pattern of expression of laterality genes in embryos depleted of Coco protein is therefore consistent with derepression of nodal signaling on the right side.

Table 4
Expression of laterality markers *Pitx2c* and *Xnr1* in Coco RNA injected embryos

Injection	Amount RNA (pg)	Injection site	Normal (%)	Bilateral (%)	Inverted (%)	Absent (%)	Total injected
Pitx2c							
Controls	0		100	0	0	0	20
Coco RNA	10	Left dorsal	0	0	4.5	95.5	22
Xnr1							
Controls	0		100	0	0	0	20
Coco RNA	10	Left dorsal	0	0	0	100	21

Injections were done at four-cell stage. Normal expression for all markers (indicated in bold first column) is in the left lateral plate mesoderm.

Table 5
Phenotypes of Xnr1 MO-injected embryos

Injection	Amount MO (ng MO)	Injection site	Situs solitus (%)	Situs ambiguus (%)	Situs inversus (%)	Total injected
Controls	0		92	7	1	87
Xnr1 MO	2	Left dorsal	27	54	19	74
Xnr1 MO	2	Right dorsal	95	5	0	38
Xnr1 Mut MO	2	Left dorsal	97	3	0	29

Injections were done at four-cell stage.

Coco is required exclusively on the right side of Xenopus embryos

We next asked if the requirement for Coco protein was side-specific. Depletion of Coco protein led to strong randomization of the left–right axis only when Coco MO was targeted to the right dorsal blastomere at the four-cell stage (28% normal embryos for right side injections, 88% normal for left side injections, Table 3). Conversely, gain of function experiments using a small amount of *Coco* RNA resulted in the reverse outcome (Table 3), with right side injections having no phenotype (81% normal), and left injections displaying a strong effect on the left–right axis (17% normal). At the molecular level, overexpression of *Coco* RNA on the left side led to loss of expression of the left side markers *Pitx2c* (95.5%, Fig. 4B, Table 4) and *Xnr1* (100%, Fig. 4D, Table 4), consistent with a decrease in TGF-β signaling. For *Xnr1,* only the anterior LPM expression was lost, whereas the posterior bilateral expression was maintained (arrowheads Figs. 4C, D). Taken together, these observations strongly suggest that Coco activity is necessary for proper left–right patterning only on the right side.

Xnr1 is required only on the left side for normal left–right patterning and is epistatic to Coco

Xnr1 has been shown to randomize the left–right axis when overexpressed on the right side (Hanafusa et al., 2000; Hyatt et al., 1996; Hyatt and Yost, 1998; Sampath et al., 1997). It was recently reported that Xnr1 MO randomize the left–right axis by suppressing expression of laterality markers when injected on the left, but not the right side of four cell stage embryos (Toyoizumi et al., 2005). Using a slightly different MO (Fig. S1 A, B), we obtained similar results (Tables 5 and 6), which suggest that Xnr1 activity is only required on the left side.

These observations, in addition to the known interaction of Coco and Xnr1 proteins (Bell et al., 2003), prompted us to ask if there is an epistatic relationship between these two secreted factors in the context of left–right patterning. Simultaneous loss of function of Coco and Xnr1 on the right side led to a significant rescue of the left–right axis phenotype seen in Coco-depleted embryos (from 42% normal embryos with Coco MO, to 82% in Coco MO+Xnr1 MO coinjected embryos, Table 7). In contrast, there was no rescue of the effect of left side Xnr1 depletion by simultaneous depletion of Coco (Table 7). These experiments prove that Xnr1 is epistatic to Coco on both sides of the embryo, and that Xnr1 activity is bilateral in the absence of Coco, but in wild-type conditions it is limited to the left side by Coco inhibition on the right.

Xnr1 is expressed bilaterally in posterior paraxial mesoderm from stage 16 (Fig. 1), and in the left lateral plate mesoderm from stage 20. To differentiate the effect of Xnr1 MO on paraxial mesoderm and lateral plate, we rescued the phenotype with Smad2, the downstream component of the nodal pathway (Massague et al., 2005). An inducible activated Smad2, *GRVP16hSmad2Δ3* (Fig. S2), was coinjected with Xnr1 MO in the dorsal left blastomere of four-cell stage embryos, or injected separately in the lateral side of the ventral left blastomere (Table 8). Dorsal injections target the axial and paraxial mesoderm at neurula stage (Figs. S3, A–D), whereas ventro-lateral injections target the lateral mesoderm (Figs. S3, E, F). Therefore, dorsal injections of inducible *Smad2* mimic paraxial nodal signaling, whereas ventro-lateral injections mimic the lateral plate signal. The best rescue was seen in ventro-lateral RNA injections, even when dexamethasone was added at stage 26 (65% normal, versus 14% without induction). When RNA was injected dorsally, heart looping was rescued only when induction happened at stage 12 (18% heart inversion, versus 47% inversion in uninduced embryos) or 18 (10% heart

Table 6
Expression of laterality markers *Pitx2c* and *Xnr1* in Xnr1 MO-injected embryos

Injection	Amount MO (ng)	Injection site	Normal (%)	Bilateral (%)	Inverted (%)	Absent (%)	Total injected
Pitx2c							
Controls	0		100	0	0	0	14
Xnr1 MO	2	Left dorsal	33	0	0	67	15
Xnr1 Mut MO	2	Left dorsal	91	0	0	9	22
Xnr1							
Controls	0		91	0	0	9	23
Xnr1 MO	2	Left dorsal	13	0	22	65	23
Xnr1 Mut MO	2	Left dorsal	100	0	0	0	30

Injections were done at four-cell stage. Normal expression for both markers (indicated in bold, first column) is in the left lateral plate mesoderm.

Table 7
Xnr1 is epistatic to Coco

Injection	Amount MO (ng MO)	Injection site	Situs solitus (%)	Situs ambiguus (%)	Situs inversus (%)	Heart inv. (%)	Gut inv (%)	Total injected
Controls	0		100	0	0	0	0	48
Coco MO	3	Right dorsal	42	12	46	54	50	52
CocoMO+Xnr1MO	3+2	Right dorsal	82	9	9	18	9	44
Xnr1 MO	2	Left dorsal	23	40	37	58	56	43
Xnr1MO+CocoMO	3+2	Left dorsal	13	45	42	55	73	67

Injections were done at four-cell stage.

inversion). This suggests that Smad2 rescues Xnr1 depletion, and that the paraxial nodal signal is effective only in neurula.

derrière is necessary for correct left–right patterning

Similar to *Xnr1*, overexpression of *derrière* RNA on the right side and a dominant negative derrière cleavage mutant overexpressed on the left side randomize the left–right axis (Chen et al., 2004; Hanafusa et al., 2000). This evidence, in addition to our observation that the gene is coexpressed in the paraxial mesoderm with *Coco* and *Xnr1*, prompted us to investigate a possible role for *derrière* in left–right patterning by specific loss of function. We tested the effect of derrière knock-down on the left–right axis. The Der MO we designed was complementary to both *derrière* sequences in the database (accession numbers AF065135 and BC073508), and interfered specifically with derrière translation in an in vitro system (Figs. S1 C, D). Injections in the dorsal left cell of four-cell stage embryos (Figs. 5A, B, Table 9) randomized the left–right axis (16% normal embryos), whereas injections with the mutated Der Mut MO, or right side injections with Der MO had little effect. Like Xnr1, derrière was epistatic to Coco (Table 10), as the phenotype seen with Coco MO injected on the right side (12.5% normal embryos) was rescued by coinjecting Der MO (79% normal). In contrast, the effect of derrière depletion on the left side was not affected by coinjecting Coco MO, as expected if derrière had been epistatic to Coco (Table 10). The laterality markers *Pitx2c* and *Xnr1* (Figs. 5C–F, Table 11) were absent in most embryos injected with Der MO on the left side (67% for *Pitx2c*, 53% for *Xnr1*), although a minority had right-sided expression. Therefore, while *derrière* expression, unlike that of *Xnr1*, is restricted to the posterior paraxial mesoderm, it shares with *Xnr1* an exclusive left side requirement for normal left–right patterning.

The specificity of this effect was demonstrated by rescue with two constructs, plasmid DNA encoding a 5′ mutated *derrière* (Table 12, *proAct-Der* DNA decreased heart inversion from 48% to 17.5%), and *GRVP16hSmad2Δ3* RNA. Rescue with dorsal RNA coinjection was time-dependent, as induction was most effective in restoring normal heart looping at stages 12 (heart inversion decreased from 61% without induction, to 23%), and 18 (20% heart inversion). We conclude that *derrière* and *Xnr1* are both part of a TGF-β cascade that, together with Coco, determines the left–right axis.

Role of derrière in the TGF-β cascade controlling the left–right axis

To address the role of *derrière* in left–right patterning, we first used animal cap assays to test the ability of *derrière* to induce expression of other TGF-β ligands and of *Coco* (Fig. 6A). In early caps (stage 10), *derrière* RNA induced all nodal-type ligands tested, *Xnr1*, *2*, *5*, *6* (Fig. 6A lanes 5, 6), and repressed expression of *Coco* (Fig. 6A lanes 4, 5). In late caps, *derrière* RNA strongly and selectively induced *Xnr1* (Fig. 6A lane 10).

We next tested in cap assays if Coco could act as an inhibitor of derrière activity (Fig. 6B). Because *derrière* can induce mesodermal genes by an indirect mechanism (Xanthos et al., 2001), we looked at the induction of nodal genes. *Coco* RNA inhibited *derrière*-induced expression of all *Xnr* genes (Fig. 6B lanes 5, 6).

To investigate a direct interaction between Coco and derrière, we coimmunoprecipitated TGF-β ligands (HA-tagged Xnr1 and

Table 8
The phenotype of Xnr1 MO-injected embryos is rescued by inducible Smad2

Injection	Amount MO (ng MO)	Injection site	Situs solitus (%)	Situs ambiguus (%)	Situs inversus (%)	Heart inv. (%)	Gut inv (%)	Total injected
Control	0		88	9	3	3	9	34
sXnr1 MO	2	Left	7	62.5	30.5	32	60	56
Xnr1MO+	2	Left	14	59	27	47	65	49
Smad2RNA		Left						
Dex. St. 12	2	Left	25	64	11	18	57	44
Dex. St. 18	2	Left	18	75	7	10	72	51
Dex. St. 26	2	Left	33	39	28	51	45	49
RNA lat	2	Left	65	30	5	9	27	23

RNA for *GRVP16hSmad2Δ3* (25 pg) was coinjected with Xnr1 MO in the dorsal left blastomere and induced at stages 12, 18, or 26, or injected separately in the left ventral blastomere (RNA lat.) and induced at stage 26. Heart looping was rescued in coinjections of MO and RNA when induction happened at stages 12 or 18, and both gut coiling and heart looping were rescued by lateral injections of RNA.

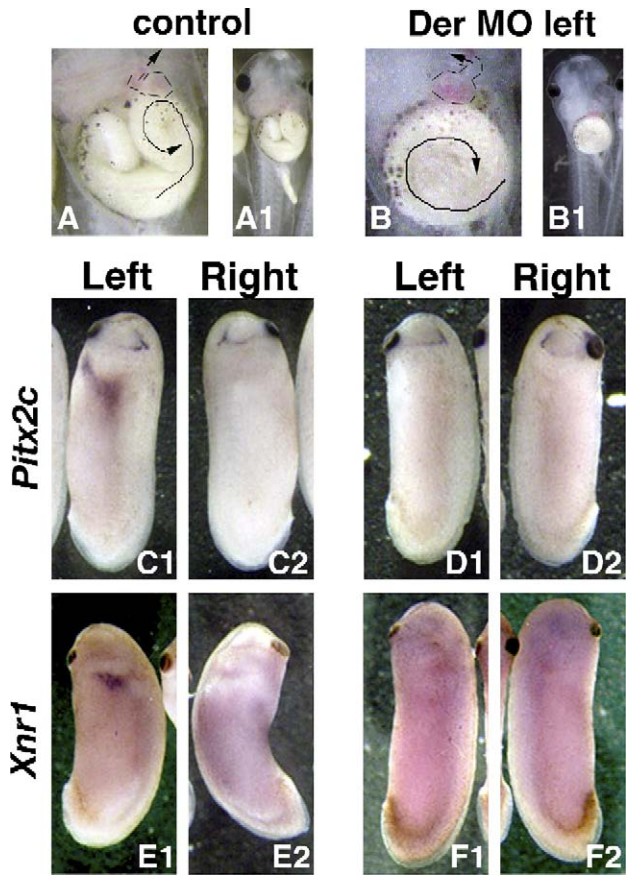

Fig. 5. Depletion of Der protein on the left side randomizes the left–right axis. Embryos were injected at the four-cell stage with 2 ng Der MO in the dorsal left blastomere, and collected at stage 46 for phenotype, or 25 for marker expression. (A, B) Stage 46 embryos, ventral view. (A) Control, (B) Xnr1 MO injected (Situs inversus). Panels A1 and B1 show the normal head and trunk of the same embryos. The contour of the hearts is indicated, and arrows show the direction of the outflow tract of the heart and of gut looping. (C–F) Effect of Der MO on expression of *Pitx2c* (C, D) and *Xnr1* (E, F). Left and right sides of the same embryos are shown. Embryos injected with Der MO are devoid of *Xnr1* and *Pitx2c* expression in the anterior left LPM (D, F).

derrière) with Coco-FLAG (Fig. 6C). Immunoprecipitation with FLAG antibodies showed that HA-tagged Xnr1 (Fig. 6C, right panel, lane 6) and derrière (Fig. 6C, left panel, lane 3) bind to FLAG-tagged Coco. This indicates a biochemical interaction between Coco and both Xnr1 and derrière.

We tested an in vivo role for derrière in *Xnr1* and *Coco* expression by injecting Der MO bilaterally in the dorsal blastomeres of four-cell embryos (Figs. 6D). At neurula stage, RT-PCR on posterior dorsal mesoderm showed a decrease in *Xnr1* expression, while *Coco* expression was unaffected (Fig. 6D, upper panel, lane 5). There was no effect of Der MO on *Xnr1* expression at stage 10 (Fig. 6D, lower panel), indicating that the decreased *Xnr1* expression in neurula was not a secondary result of an early interaction between the two genes. Xnr1 MO had no effect on either gene (Fig. 6D, upper panel, lane 4). In conclusion, derrière is required to maintain a higher level of *Xnr1* expression at neurula stage.

Discussion

We report here that the DAN domain protein Coco is required for left–right patterning in the *Xenopus* embryo. In addition to the previously described maternal and blastula stage expression (Bell et al., 2003), we find that *Coco*, together with *Xnr1* and *derrière*, is expressed in the posterior paraxial mesoderm. Although expression of the three genes is essentially symmetrical at all stages, Coco is required only on the right side, while the two TGF-β ligands are required only on the left. Knock-down of Coco leads to mostly bilateral expression of left side markers, the likely cause for the randomized left–right axis phenotype. Both derrière and Xnr1 are required for the left signal, and both interact functionally and biochemically with Coco.

We have uncovered novel properties for Coco, with potential impact on the existing models for generating left–right asymmetry. Unlike its ortholog in mice and zebrafish, *Coco* is a maternal gene, and its RNA is localized to the animal half of early embryos. This first stage of expression ends at the beginning of gastrulation, when RNA levels decrease precipitously (Bell et al., 2003). From stage 13, *Coco* reappears on the ventral side of the posterior paraxial mesoderm, around an area (the inner side of the upper dorsal lip) reported to have ciliated cells and to express left–right dynein (Essner et al., 2002). This area is comparable to the node of the mouse and to Kupffer's vesicle in zebrafish, both involved in establishing the left–right axis (Essner et al., 2005; Marszalek et al., 1999; Nonaka et al., 1998; Supp et al., 1997). Similar to the expression of *Charon* in zebrafish and to the early expression of *Dand5/Cerl-2/Dte* in mouse (Hashimoto et al., 2004; Marques et al., 2004), *Coco* does not show a systematic left–right bias (Fig. 1). We also demonstrate that *Coco* overlaps the expression of *Xnr1* (Fig. 1), in contrast with the nonoverlapping pattern reported in zebrafish (Hashimoto et al., 2004). While it is tempting to assign the observed phenotypes to direct interference with expression of Coco and TGF-β ligands in the posterior mesoderm, we cannot rule out an earlier effect on protein expression. A partial overlap in expression pattern is seen around the start of gastrulation in the dorsal marginal zone, but

Table 9
Phenotypes of Der MO-injected embryos

Injection	Amount MO (ng MO)	Injection site	Situs solitus (%)	Situs ambiguus (%)	Situs inversus (%)	Total injected
Controls	0		92	8	0	88
Der MO	2	Left dorsal	16	48	36	56
Der MO	2	Right dorsal	76	24	0	56
Der Mut MO	2	Left dorsal	79	17	4	46

Injections were done at four-cell stage.

Table 10
derrière is epistatic to Coco

Injection	Amount MO (ng MO)	Injection site	Situs solitus (%)	Situs ambiguus (%)	Situs inversus (%)	Total injected
Controls	0		96	4	0	52
Coco MO	3	Right dorsal	12.5	42.5	45	40
Coco MO+Der MO	3+2	Right dorsal	79	16	5	38
Der MO	2	Left dorsal	20	34	46	35
Coco MO+Der MO	3+2	Left dorsal	31	24	45	42

Injections were done at four-cell stage.

Coco is mostly animal, while *Xnr1* and *derrière* are dorsal marginal and endodermal only (Bell et al., 2003; Jones et al., 1995; Sun et al., 1999). We also found that Coco MO injections decreased Coco protein in the posterior mesoderm at stage 18 (Fig. 2), but did not change expression of midline markers (*Xlefty-a*, *Shh*, *Zic3*) or posterior paraxial genes (*Der*, *Xnr1*), which make an indirect effect on left–right axis due to defective mesodermal specification/patterning appear unlikely. Therefore, based on expression patterns, unchanged gene expression before stage 20, and data from other vertebrates on the importance of posterior mesoderm in left–right patterning, the place and time for Coco, Xnr1 and derrière to interact in regulating the left–right axis is more likely the posterior mesoderm at neurula stage.

On the functional side, the most important finding reported here is the exclusive requirement for Coco on the right side of the embryo. Even when either derrière or Xnr1 are depleted on the left, simultaneous depletion of Coco on the same side is still without effect. The phenotype of right side depletion of Coco protein (Fig. 2, Table 1) is rescued by concomitantly depleting Xnr1 or derrière protein (Tables 7 and 10). Thus, embryos lacking both one of the TGF-β ligands and its inhibitor on the right side are normal. Together with the bilateral expression of laterality markers observed with Coco MO (Fig. 3, Table 2), the epistasis experiments demonstrate that, in the absence of Coco, the nodal signal is bilateral, and the TGF-β ligands expressed on the right side do not normally signal because of inhibition by Coco.

We show for the first time, by using a loss of function approach with specific MOs, that endogenous *derrière* is required for the left side signal (Figs. 5, 6, Tables 9 and 11). The similar Xnr1 depletion experiments confirm recently reported results (Toyoizumi et al., 2005). While expression of *Xnr1* in the posterior paraxial mesoderm was previously reported (Lohr et al., 1998; Lustig et al., 1996; Onuma et al., 2005), the expression of *derrière* (Sun et al., 1999) in the same region is first reported here (Fig. 1). The phenotypes of Xnr1 or derrière protein depletions were indistinguishable, and were rescued by an inducible Smad2 (Tables 8 and 12). Derrière appears to be the upstream factor, as shown by the timing of its expression, its ability to induce selectively *Xnr1* in late animal caps, and the effect of derrière depletion on *Xnr1* expression (Fig. 6). This makes *derrière* the likely homologue of mouse *GDF1*, although the latter is also expressed outside the posterior paraxial mesoderm (Rankin et al., 2000; Zhang et al., 2001). The two genes, coexpressed in the posterior paraxial mesoderm, could form a TGF-β signaling relay, with *derrière* transmitting the original signal, which is then conveyed by *Xnr1*. Our data are in agreement with a recent report on the role of XCR2, an EGF-CFC molecule and coreceptor for nodal signaling, which is required for left–right patterning only on the left side (Onuma et al., 2005).

The timing of Coco inhibition can be deduced indirectly from the timing of the nodal-like signal required in left–right determination. Injections of ligands like activin and TGF-β5 in the LPM (Lohr et al., 1997; Mogi et al., 2003) induced *Xnr1* as late as the end of neurula stage (stage 20), and the Xnr1 target genes *antivin/Xlefty-b* and *Pitx2* were induced even when embryos were injected at tadpole stage. Our timed rescues of the paraxial mesoderm depletions of Xnr1 and derrière with an inducible Smad2 (Tables 8 and 12) indicate that Coco has to be active on the right side at least until stage 18. The fact that Smad induction is effective at a later stage in lateral versus dorsal injections reflects an earlier requirement for nodal signal in the paraxial mesoderm than in the LPM, similar to what has been described in the mouse (Brennan et al., 2002; Saijoh et al., 2003).

Is Coco a regulated or a default component of the left–right cascade? On the right side, Coco is necessary to block the nodal signal. What happens on the left side is far less clear. It has been

Table 11
Expression of laterality markers *Pitx2c* and *Xnr1* in Der MO-injected embryos

Injection	Amount MO (ng)	Injection site	Normal (%)	Bilateral (%)	Inverted (%)	Absent (%)	Total injected
Pitx2c							
Controls	0		100	0	0	0	14
Der MO	2	Left dorsal	33	0	0	67	15
Der Mut MO	2	Left dorsal	91	0	0	9	22
Xnr1							
Controls	0		100	0	0	0	13
Der MO	2	Left dorsal	28	5	14	53	21
Der Mut MO	2	Left dorsal	96	4	0	0	23

Injections were done at four-cell stage. Normal expression for all markers (indicated in bold, first column) is in the left lateral plate mesoderm.

Table 12
The phenotype of Der MO-injected embryos is rescued by inducible Smad2

Injection	Amount MO (ng MO)	Injection site	Situs solitus (%)	Situs ambiguus (%)	Situs inversus (%)	Heart inv. (%)	Gut inv (%)	Total
Controls	0		98.8	1.2	0	0	1.2	83
Der MO	2	Left dorsal	23	49	28	48	57	90
DerMO+Smad2RNA	2	Left dorsal	11	54	35	61	63	54
Dex. St. 12	2	Left dorsal	36	41	23	23	64	44
Dex. St. 18	2	Left dorsal	36	44	20	20	65	34
Dex. St. 26	2	Left dorsal	33	41	26	30	63	46
Der MO+Der Mut DNA	2	Left dorsal	32.5	55	12.5	17.5	60	40

Smad2RNA is *GRVP16hSmad2Δ3* (25 pg). *Der Mut* DNA is the *proAct Der* plasmid. Injections were done at four-cell stage.

suggested (Hashimoto et al., 2004) that this class of inhibitors would set a threshold for nodal, which could be overcome on the left but not on the right. In this model, the DAN domain protein would have a symmetric activity and the difference between left and right would have to be the result of higher activity of nodal on the left. Because in zebrafish, like in *Xenopus*, expression of the *nodal* homologue in paraxial mesoderm is not increased on the left, the mechanism would have to be posttranscriptional, affecting protein level or function. In an alternative model, similarly based on posttranscriptional regulation, Coco activity

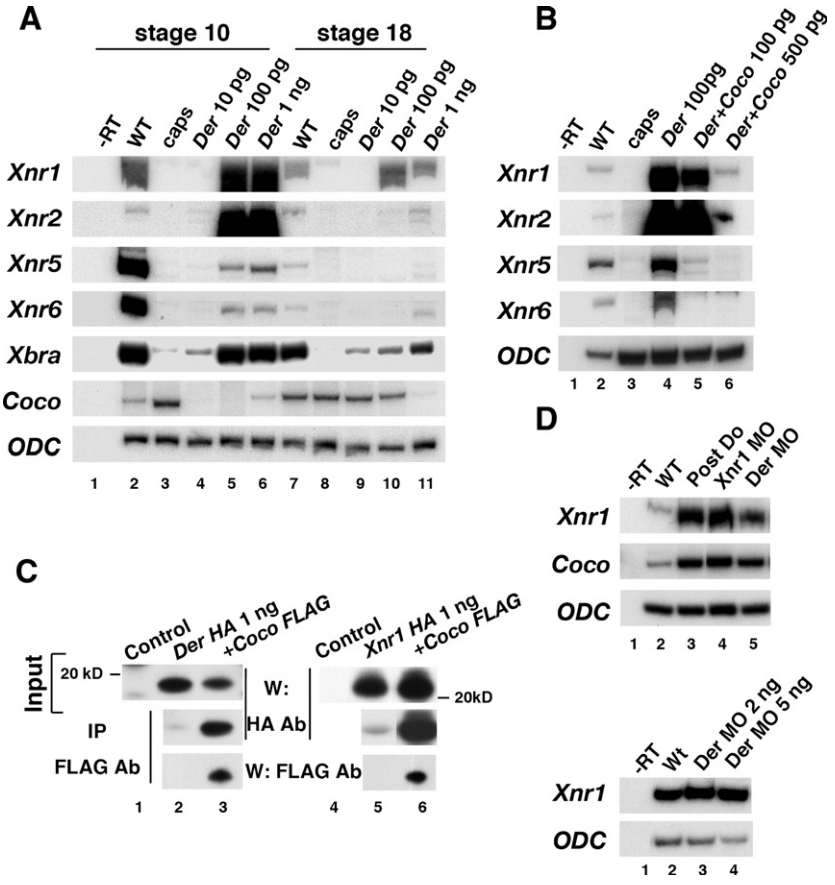

Fig. 6. *derrière*, *Xnr-1*and *Coco* interact functionally and biochemically. (A) *derrière* specifically induces *Xnr1* expression in neurula. RT-PCR of animal caps from embryos injected with *derrière* RNA, recovered at gastrula stage 10 (lanes 2–6) or neurula stage 18 (lanes 7–11). *Xnr1* is specifically induced by *derrière* RNA at stage 18 (lane 10), and *coco* is inhibited at both early (lanes 4, 5), and late stage (lanes 10, 11). *Xbra* expression indicates mesoderm induction, *ODC* is the loading control. (B) *Coco* inhibits the effects of *derrière*. RT-PCR of animal caps (stage 10) injected with the indicated RNAs. *Coco* RNA inhibits induction of *nodal* genes by 100 pg *derrière* RNA (lane 5, 6). (C) Coco and derrière interact biochemically. *HA-derrière* or *HA-Xnr1* (1 ng RNA), with or without 100 pg *FLAG-Coco* RNA, were injected in the animal poles of four-cell stage embryos. Secreted proteins were immunoprecipitated from cap cell medium with anti-FLAG antibody beads and analyzed by Western blot. Top: input of HA-derrière (left panel) and HA-Xnr1 (right panel), anti-HA blot (control lanes are supernatants of cells expressing the other ligand); middle: IP-ed proteins, anti-HA blot, both derrière and Xnr1 are detected only when FLAG-Coco is coexpressed (lanes 2, 5 ligands alone; lanes 3, 6 ligands with FLAG Coco); bottom: IP-ed proteins, anti-FLAG blot for FLAG-Coco. (D) Upper panel. Der MO decreases *Xnr1* expression in posterior mesoderm. RT-PCR of the posterior dorsal fragments of stage 18 embryos, injected bilaterally on the dorsal side with the indicated MOs (2 ng in each blastomere). *Xnr1* is decreased by Der MO (lane 5), but not by Xnr1 MO (lane 4). Lower panel. Der MO has not effect on expression of *Xnr1* in stage 10 embryos. RT-PCR of stage 10 embryos (dorsal halves) injected bilaterally on the dorsal side with 2 and 5 ng Der MO.

would be decreased on the left, or increased on the right, by a decrease in protein levels or function. The data presented here are compatible with both models.

In conclusion, we describe a TGF-β cascade formed by *derrière* and *Xnr1* in the posterior paraxial mesoderm of neurula-stage *Xenopus* embryos, regulated by the DAN domain protein Coco. Correct determination of the left–right axis requires TGF-β ligands exclusively on the left side, and Coco exclusively on the right. These factors, possibly under posttranscriptional control, interact to generate a TGF-β signal limited to the left side of the embryo.

Acknowledgments

We thank F. Spagnoli and A. Levine for comments. Plasmids were provided by Drs. J. Aruga, M. Asashima, M. Blum, R. Harland, M. Kato, J. Massagué, A. Ruiz i Altaba, P. Wilson, C. Wright, and H. Joseph Yost. This work was supported by the NICHD fellowship 1F32 HD40724 to A. Vonica, and by NIH grant HD32105 to A.H.B.

Appendix A. Supplementary data

Supplementary data associated with this article can be found, in the online version, at doi:10.1016/j.ydbio.2006.09.039.

References

Altschul, S.F., Gish, W., Miller, W., Myers, E.W., Lipman, D.J., 1990. Basic local alignment search tool. J. Mol. Biol. 215, 403–410.

Avsian-Kretchmer, O., Hsueh, A.J., 2004. Comparative genomic analysis of the eight-membered ring cysteine knot-containing bone morphogenetic protein antagonists. Mol. Endocrinol. 18, 1–12.

Bell, E., Munoz-Sanjuan, I., Altmann, C.R., Vonica, A., Brivanlou, A.H., 2003. Cell fate specification and competence by Coco, a maternal BMP, TGFbeta and Wnt inhibitor. Development 130, 1381–1389.

Bisgrove, B.W., Yost, H.J., 2001. Classification of left–right patterning defects in zebrafish, mice, and humans. Am. J. Med. Genet. 101, 315–323.

Brand, T., 2003. Heart development: molecular insights into cardiac specification and early morphogenesis. Dev. Biol. 258, 1–19.

Branford, W.W., Essner, J.J., Yost, H.J., 2000. Regulation of gut and heart left–right asymmetry by context-dependent interactions between *Xenopus* lefty and BMP4 signaling. Dev. Biol. 223, 291–306.

Brennan, J., Norris, D.P., Robertson, E.J., 2002. Nodal activity in the node governs left–right asymmetry. Genes Dev. 16, 2339–2344.

Chang, C., Wilson, P.A., Mathews, L.S., Hemmati-Brivanlou, A., 1997. A *Xenopus* type I activin receptor mediates mesodermal but not neural specification during embryogenesis. Development 124, 827–837.

Chen, Y., Mironova, E., Whitaker, L.L., Edwards, L., Yost, H.J., Ramsdell, A.F., 2004. ALK4 functions as a receptor for multiple TGF beta-related ligands to regulate left–right axis determination and mesoderm induction in *Xenopus*. Dev. Biol. 268, 280–294.

Cheng, A.M., Thisse, B., Thisse, C., Wright, C.V., 2000. The lefty-related factor Xatv acts as a feedback inhibitor of nodal signaling in mesoderm induction and L–R axis development in *Xenopus*. Development 127, 1049–1061.

Collignon, J., Varlet, I., Robertson, E.J., 1996. Relationship between asymmetric nodal expression and the direction of embryonic turning [see comment]. Nature 381, 155–158.

Conlon, F.L., Lyons, K.M., Takaesu, N., Barth, K.S., Kispert, A., Herrmann, B., Robertson, E.J., 1994. A primary requirement for nodal in the formation and maintenance of the primitive streak in the mouse. Development 120, 1919–1928.

Darken, R.S., Wilson, P.A., 2001. Axis induction by wnt signaling: target promoter responsiveness regulates competence. Dev. Biol. 234, 42–54.

Eimon, P.M., Harland, R.M., 2002. Effects of heterodimerization and proteolytic processing on Derriere and Nodal activity: implications for mesoderm induction in *Xenopus*. Development 129, 3089–3103.

Ekker, S.C., McGrew, L.L., Lai, C.J., Lee, J.J., von Kessler, D.P., Moon, R.T., Beachy, P.A., 1995. Distinct expression and shared activities of members of the hedgehog gene family of *Xenopus laevis*. Development 121, 2337–2347.

Essner, J.J., Vogan, K.J., Wagner, M.K., Tabin, C.J., Yost, H.J., Brueckner, M., 2002. Conserved function for embryonic nodal cilia [see comment]. Nature 418, 37–38.

Essner, J.J., Amack, J.D., Nyholm, M.K., Harris, E.B., Yost, H.J., 2005. Kupffer's vesicle is a ciliated organ of asymmetry in the zebrafish embryo that initiates left–right development of the brain, heart and gut. Development 132, 1247–1260.

Hanafusa, H., Masuyama, N., Kusakabe, M., Shibuya, H., Nishida, E., 2000. The TGF-beta family member derriere is involved in regulation of the establishment of left–right asymmetry. EMBO Rep. 1, 32–39.

Harland, R.M., 1991. In situ hybridization: an improved whole-mount method for *Xenopus* embryos. Methods Cell Biol. 36, 685–695.

Hashimoto, H., Rebagliati, M., Ahmad, N., Muraoka, O., Kurokawa, T., Hibi, M., Suzuki, T., 2004. The Cerberus/Dan-family protein Charon is a negative regulator of Nodal signaling during left–right patterning in zebrafish. Development 131, 1741–1753.

Hemmati-Brivanlou, A., Melton, D.A., 1992. A truncated activin receptor inhibits mesoderm induction and formation of axial structures in *Xenopus* embryos [see comment]. Nature 359, 609–614.

Hsu, D.R., Economides, A.N., Wang, X., Eimon, P.M., Harland, R.M., 1998. The *Xenopus* dorsalizing factor Gremlin identifies a novel family of secreted proteins that antagonize BMP activities. Mol. Cell 1, 673–683.

Hyatt, B.A., Yost, H.J., 1998. The left–right coordinator: the role of Vg1 in organizing left–right axis formation. Cell 93, 37–46.

Hyatt, B.A., Lohr, J.L., Yost, H.J., 1996. Initiation of vertebrate left–right axis formation by maternal Vg1. Nature 384, 62–65.

Jones, C.M., Kuehn, M.R., Hogan, B.L., Smith, J.C., Wright, C.V., 1995. Nodal-related signals induce axial mesoderm and dorsalize mesoderm during gastrulation. Development 121, 3651–3662.

Kitaguchi, T., Nagai, T., Nakata, K., Aruga, J., Mikoshiba, K., 2000. Zic3 is involved in the left–right specification of the *Xenopus* embryo. Development 127, 4787–4795.

Kolker, S.J., Tajchman, U., Weeks, D.L., 2000. Confocal imaging of early heart development in *Xenopus laevis*. Dev. Biol. 218, 64–73.

Levin, M., 2005. Left–right asymmetry in embryonic development: a comprehensive review. Mech. Dev. 122, 3–25.

Liu, F., Pouponnot, C., Massague, J., 1997. Dual role of the Smad4/DPC4 tumor suppressor in TGFbeta-inducible transcriptional complexes. Genes Dev. 11, 3157–3167.

Lohr, J.L., Danos, M.C., Yost, H.J., 1997. Left–right asymmetry of a nodal-related gene is regulated by dorsoanterior midline structures during *Xenopus* development. Development 124, 1465–1472.

Lohr, J.L., Danos, M.C., Groth, T.W., Yost, H.J., 1998. Maintenance of asymmetric nodal expression in *Xenopus laevis*. Dev. Genet. 23, 194–202.

Long, S., Ahmad, N., Rebagliati, M., 2003. The zebrafish nodal-related gene southpaw is required for visceral and diencephalic left–right asymmetry. Development 130, 2303–2316.

Lustig, K.D., Kroll, K., Sun, E., Ramos, R., Elmendorf, H., Kirschner, M.W., 1996. A *Xenopus* nodal-related gene that acts in synergy with noggin to induce complete secondary axis and notochord formation. Development 122, 3275–3282.

Marques, S., Borges, A.C., Silva, A.C., Freitas, S., Cordenonsi, M., Belo, J.A., 2004. The activity of the Nodal antagonist Cerl-2 in the mouse node is required for correct L/R body axis. Genes Dev. 18, 2342–2347.

Marszalek, J.R., Ruiz-Lozano, P., Roberts, E., Chien, K.R., Goldstein, L.S., 1999. Situs inversus and embryonic ciliary morphogenesis defects in mouse mutants lacking the KIF3A subunit of kinesin-II. Proc. Natl. Acad. Sci. U. S. A. 96, 5043–5048.

Massague, J., Seoane, J., Wotton, D., 2005. Smad transcription factors. Genes Dev. 19, 2783–2810.

Mogi, K., Goto, M., Ohno, E., Azumi, Y., Takeuchi, S., Toyoizumi, R., 2003. *Xenopus* neurula left–right asymmetry is respecified by microinjecting TGF-beta5 protein. Int. J. Dev. Biol. 47, 15–29.

Neubuser, A., Koseki, H., Balling, R., 1995. Characterization and developmental expression of Pax9, a paired-box-containing gene related to Pax1. Dev. Biol. 170, 701–716.

Nieuwkoop, P.D., Faber, J., 1967. Normal Table of *Xenopus laevis*. North Holland Publishing Co, Amsterdam, The Netherlands.

Nonaka, S., Tanaka, Y., Okada, Y., Takeda, S., Harada, A., Kanai, Y., Kido, M., Hirokawa, N., 1998. Randomization of left–right asymmetry due to loss of nodal cilia generating leftward flow of extraembryonic fluid in mice lacking KIF3B motor protein [erratum appears in Cell 1999 Oct 1;99(1):117]. Cell 95, 829–837.

Onuma, Y., Yeo, C.-Y., Whitman, M., 2005. XCR2, one of three *Xenopus* EGF-CFC genes, has a distinct role in the regulation of left–right patterning. Development 133, 237–250.

Pearce, J.J., Penny, G., Rossant, J., 1999. A mouse cerberus/Dan-related gene family. Dev. Biol. 209, 98–110.

Piccolo, S., Agius, E., Leyns, L., Bhattacharyya, S., Grunz, H., Bouwmeester, T., De Robertis, E.M., 1999. The head inducer Cerberus is a multifunctional antagonist of Nodal, BMP and Wnt signals. Nature 397, 707–710.

Piedra, M.E., Ros, M.A., 2002. BMP signaling positively regulates Nodal expression during left right specification in the chick embryo. Development 129, 3431–3440.

Rankin, C.T., Bunton, T., Lawler, A.M., Lee, S.J., 2000. Regulation of left–right patterning in mice by growth/differentiation factor-1. Nat. Genet. 24, 262–265.

Rodriguez Esteban, C., Capdevila, J., Economides, A.N., Pascual, J., Ortiz, A., Izpisua Belmonte, J.C., 1999. The novel Cer-like protein Caronte mediates the establishment of embryonic left–right asymmetry [see comment]. Nature 401, 243–251.

Ruiz i Altaba, A., Jessell, T.M., Roelink, H., 1995. Restrictions to floor plate induction by hedgehog and winged-helix genes in the neural tube of frog embryos. Mol. Cell. Neurosci. 6, 106–121.

Saijoh, Y., Oki, S., Ohishi, S., Hamada, H., 2003. Left–right patterning of the mouse lateral plate requires nodal produced in the node. Dev. Biol. 256, 160–172.

Sampath, K., Cheng, A.M., Frisch, A., Wright, C.V., 1997. Functional differences among *Xenopus* nodal-related genes in left–right axis determination. Development 124, 3293–3302.

Schlange, T., Arnold, H.H., Brand, T., 2002. BMP2 is a positive regulator of Nodal signaling during left–right axis formation in the chicken embryo. Development 129, 3421–3429.

Schweickert, A., Campione, M., Steinbeisser, H., Blum, M., 2000. Pitx2 isoforms: involvement of Pitx2c but not Pitx2a or Pitx2b in vertebrate left–right asymmetry. Mech. Dev. 90, 41–51.

Shook, D.R., Majer, C., Keller, R., 2004. Pattern and morphogenesis of presumptive superficial mesoderm in two closely related species, *Xenopus laevis* and *Xenopus tropicalis*. Dev. Biol. 270, 163–185.

Sive, H.L., Grainger, R.M., Harland, R.M., 1997. Early Development of *Xenopus laevis*.

Sun, B.I., Bush, S.M., Collins-Racie, L.A., LaVallie, E.R., DiBlasio-Smith, E.A., Wolfman, N.M., McCoy, J.M., Sive, H.L., 1999. derriere: a TGF-beta family member required for posterior development in *Xenopus*. Development 126, 1467–1482.

Supp, D.M., Witte, D.P., Potter, S.S., Brueckner, M., 1997. Mutation of an axonemal dynein affects left–right asymmetry in inversus viscerum mice. Nature 389, 963–966.

Takahashi, S., Yokota, C., Takano, K., Tanegashima, K., Onuma, Y., Goto, J., Asashima, M., 2000. Two novel nodal-related genes initiate early inductive events in *Xenopus* Nieuwkoop center. Development 127, 5319–5329.

Toyoizumi, R., Ogasawara, T., Takeuchi, S., Mogi, K., 2005. *Xenopus* nodal-related-1 is indespensable only for left–right axis determination. Int. J. Dev. Biol. 49, 923–938.

Vonica, A., Gumbiner, B.M., 2002. Zygotic Wnt activity is required for Brachyury expression in the early *Xenopus laevis* embryo. Dev. Biol. 250, 112–127.

Vonica, A., Weng, W., Gumbiner, B.M., Venuti, J.M., 2000. TCF is the nuclear effector of the beta-catenin signal that patterns the sea urchin animal-vegetal axis. Dev. Biol. 217, 230–243.

Wilson, P.A., Melton, D.A., 1994. Mesodermal patterning by an inducer gradient depends on secondary cell-cell communication. Curr. Biol. 4, 676–686.

Wright, C.V., 2001. Mechanisms of left–right asymmetry: what's right and what's left? Dev. Cell 1, 179–186.

Xanthos, J.B., Kofron, M., Wylie, C., Heasman, J., 2001. Maternal VegT is the initiator of a molecular network specifying endoderm in *Xenopus laevis*. Development 128, 167–180.

Yagi, K., Goto, D., Hamamoto, T., Takenoshita, S., Kato, M., Miyazono, K., 1999. Alternatively spliced variant of Smad2 lacking exon 3. Comparison with wild-type Smad2 and Smad3. J. Biol. Chem. 274, 703–709.

Yokouchi, Y., Vogan, K.J., Pearse, R.V., Tabin, C.J., 1999. Antagonistic signaling by Caronte, a novel Cerberus-related gene, establishes left–right asymmetric gene expression. Cell 98, 573–583.

Zhang, X.M., Ramalho-Santos, M., McMahon, A.P., 2001. Smoothened mutants reveal redundant roles for Shh and Ihh signaling including regulation of L/R symmetry by the mouse node [republished from Cell. 2001 Jun 15;105(6):781–92; PMID: 11440720]. Cell 106, 781–792.

Zhou, X., Sasaki, H., Lowe, L., Hogan, B.L., Kuehn, M.R., 1993. Nodal is a novel TGF-beta-like gene expressed in the mouse node during gastrulation. Nature 361, 543–547.

Zhu, L., Marvin, M.J., Gardiner, A., Lassar, A.B., Mercola, M., Stern, C.D., Levin, M., 1999. Cerberus regulates left–right asymmetry of the embryonic head and heart. Curr. Biol. 9, 931–938.